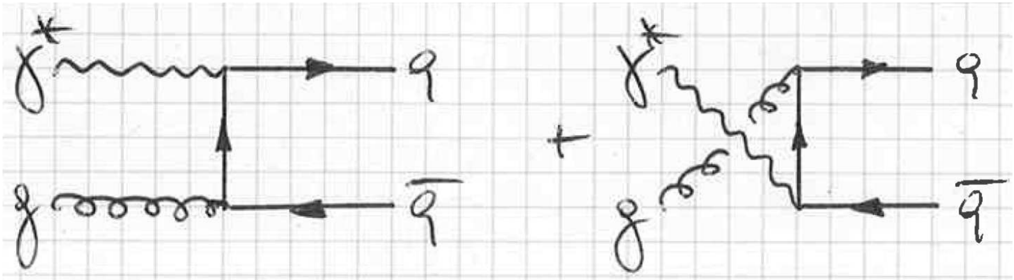

$$\delta\hat{\mathcal{F}}_L^{\gamma g} = T_R\ \frac{\alpha_s}{2\pi}\ 4z(1-z) \qquad \left[T_R = \frac{1}{2}\right]$$

$$\delta\hat{\mathcal{F}}_2^{\gamma g} = \frac{\Gamma(1-\epsilon)}{\Gamma(1-2\epsilon)}\left(\frac{4\pi\mu^2}{Q^2}\right)^{\epsilon}\left[-\frac{1}{\epsilon} - \log\frac{z}{1-z}\right]\frac{\alpha_s}{2\pi}\ P_{qg}(z) + T_R\ \frac{\alpha_s}{2\pi}\ [8z(1-z)-1]$$

$$P_{qg}(z) = T_R[z^2 + (1-z)^2]$$

gluon-spin average: $\frac{1}{2} \to \frac{1}{n-2} = \frac{1}{2(1-\epsilon)}$

DIS structure function:

$$F_2(x,Q^2) = 2x\sum_q e_q^2\left\{[q_0 + \bar{q}_0]\otimes\hat{\mathcal{F}}_2^{\gamma q} + g_0\otimes\hat{\mathcal{F}}_2^{\gamma g}\right\}$$

with the convolution:

$$f\otimes g = \int_0^1 dydz\ f(y)\ g(z)\ \delta(x-yz) = \int_x^1 \frac{dz}{z}\ f\left(\frac{x}{z}\right)g(z)$$

The remaining collinear singularities are removed by the renormalization of the parton densities.

Renormalization of the parton densities [mass factorization]:

$$q_0(x) = F_{qq} \otimes q(x,\mu_F^2) + F_{qg} \otimes g(x,\mu_F^2)$$

$$F_{ij}(x) = \delta_{ij}\delta(1-x) + \frac{\alpha_s}{2\pi}\left\{\frac{1}{\epsilon}\frac{\Gamma(1-\epsilon)}{\Gamma(1-2\epsilon)}\left(\frac{4\pi\mu^2}{\mu_F^2}\right)^{\epsilon} P_{ij}(x) - f_{ij}(x)\right\}$$

$\mu_F =$ factorization scale of the parton densities

$$\Rightarrow \mu_F^2\frac{\partial q_0(x)}{\partial \mu_F^2} = 0 = -\frac{\alpha_s}{2\pi}\left[P_{qq} \otimes q(x,\mu_F^2) + P_{qg} \otimes g(x,\mu_F^2)\right] + \mu_F^2\frac{\partial q(x,\mu_F^2)}{\partial \mu_F^2} + \mathcal{O}(\alpha_s^2)$$

$\Rightarrow q(x,\mu_F^2)$ is solution of the Alterelli–Parisi equations at LO.

Result:

$$F_2(x,Q^2) = 2x\sum_q e_q^2[q(x,\mu_F^2) + \bar{q}(x,\mu_F^2)] + \Delta F_2(x,Q^2)$$

$$\Delta F_2(x,Q^2) = 2x\frac{\alpha_s}{2\pi}\sum_q e_q^2\int_x^1\frac{dz}{z}\left\{C_F\left[q\left(\frac{x}{z},\mu_F^2\right) + \bar{q}\left(\frac{x}{z},\mu_F^2\right)\right] *\right.$$

$$* \left[-\frac{P_{qq}(z)}{C_F}\log\frac{\mu_F^2 z}{Q^2} + (1+z^2)\left(\frac{\log(1-z)}{1-z}\right)_+ - \frac{3}{2}\left(\frac{1}{1-z}\right)_+ + 3 + 2z\right.$$

$$\left. - \left(\frac{9}{2} + \frac{\pi^2}{3}\right)\delta(1-z) - \frac{f_{qq}(z)}{C_F}\right]$$

$$\left. + T_R\ g\left(\frac{x}{z},\mu_F^2\right)\left[-\frac{P_{qg}(z)}{T_R}\log\frac{\mu_F^2 z}{Q^2(1-z)} + 8z(1-z) - 1 - \frac{f_{qg}(z)}{T_R}\right]\right\}$$

$$F_L(x,Q^2) = F_2(x,Q^2) - 2x\ F_1(x,Q^2)$$

$$= 2x\frac{\alpha_s}{2\pi}\sum_q e_q^2\int_x^1\frac{dz}{z}\left\{C_F\left[q\left(\frac{x}{z},\mu_F^2\right) + \bar{q}\left(\frac{x}{z},\mu_F^2\right)\right]2z + T_R\ g\left(\frac{x}{z},\mu_F^2\right)4z(1-z)\right\}$$

PHYSICAL INTERPRETATION:

1.) natural factorization scale: $\mu_F^2 = Q^2$

2.) factorization scheme:

(i) $\overline{MS}$ scheme: $f_{ij}^{\overline{MS}}(z) \equiv 0$

(ii) DIS scheme: $F_2(x,Q^2) \equiv 2x \sum_q e_q^2 \left[q(x,Q^2) + \bar{q}(x,Q^2) \right]$

$$\Rightarrow \Delta F_2 \equiv 0 \quad [\mu_F^2 = Q^2]$$

$$\Rightarrow f_{qq}^{DIS}(z) = C_F \left\{ -\frac{1+z^2}{1-z} \log z + (1+z^2) \left(\frac{\log(1-z)}{1-z} \right)_+ - \frac{3}{2} \left(\frac{1}{1-z} \right)_+ \right.$$
$$\left. + 3 + 2z - \left(\frac{9}{2} + \frac{\pi^2}{3} \right) \delta(1-z) \right\}$$

$$f_{qg}^{DIS}(z) = T_R \left\{ [z^2 + (1-z)^2] \log \frac{1-z}{z} + 8z(1-z) - 1 \right\}$$

DIS known up to N^{3}LO [$\leftarrow$ factorization works]

FACTORIZATION THEOREM OF QCD

Partonic cross sections develop collinear divergencies in the hadronic initial (final) state that factorize universally [process-independent] from the hard scattering process and can be absorbed in the renormalized parton densities of the initial state (and fragmentation functions of the final state). These renormalized parton densities (fragmentation functions) are solutions of the DGLAP equations.

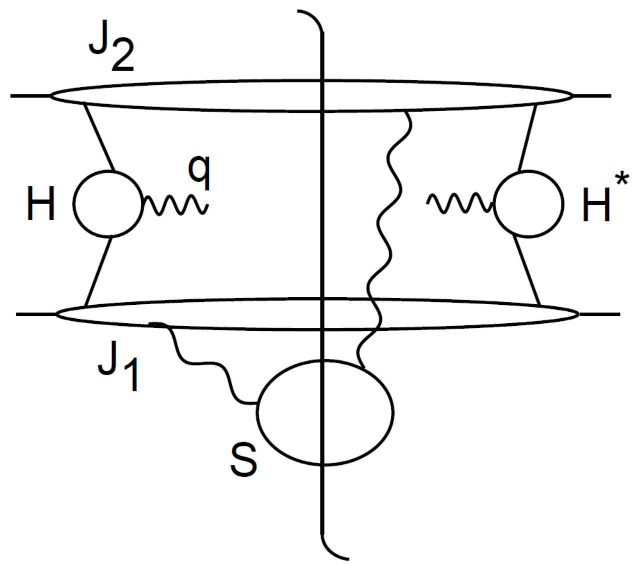

§8. Drell–Yan Processes

Production of elw. int. particles in hadron coll.

$p\bar{p} \to \mu^+\mu^- + X$

$p\bar{p} \to W^\pm, Z + X \qquad \ldots$

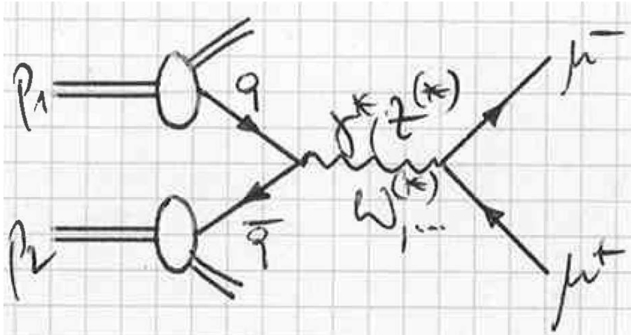

$$\frac{d\mathcal{L}^{q\bar{q}}}{d\tau} = \sum_q \int_\tau^1 \frac{dx}{x} \left[q(x)\bar{q}\left(\frac{\tau}{x}\right) + \bar{q}(x) q\left(\frac{\tau}{x}\right)\right]$$

$$\sigma = \int_{\tau_0}^1 d\tau \sum_q \frac{d\mathcal{L}^{q\bar{q}}}{d\tau}\ \hat{\sigma}(\tau s)$$

$\uparrow$ "luminosity of $q, \bar{q}$ in hadron beams"

$$M_{\mu\mu}^4 \frac{d\sigma}{dM_{\mu\mu}^2} = \frac{4\pi\alpha^2}{3N_c} \tau_\mu \sum_q e_q^2 \left.\frac{d\mathcal{L}^{q\bar{q}}}{d\tau}\right|_{\tau_\mu = \frac{M_{\mu\mu}^2}{s}}$$

QCD corrections:

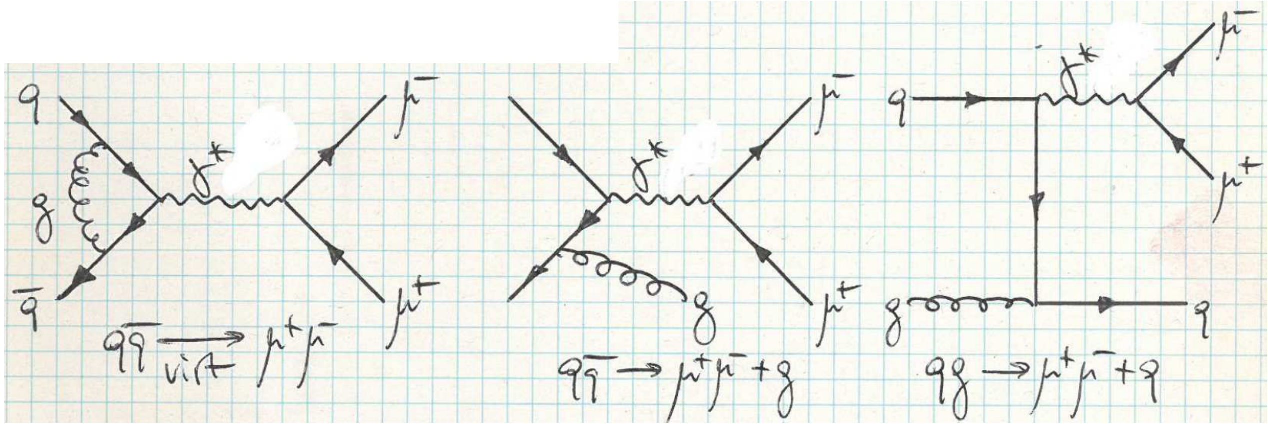

[known at NNLO]

$$M^4_{\mu\mu}\frac{d\sigma}{dM^2_{\mu\mu}} = \frac{4\pi\alpha^2}{3N_c}\tau_\mu \int_{\tau_0}^1 \frac{d\tau}{\tau}\left\{\sum_q e_q^2 \frac{d\mathcal{L}^{q\bar q}}{d\tau}\left[\delta(1-z) + \frac{\alpha_s(\mu_R^2)}{\pi}D_{qq}(z)\right]\right.$$

$$\left. + \sum_{q,\bar q} e_q^2 \frac{d\mathcal{L}^{gq}}{d\tau}\,\frac{\alpha_s(\mu_R^2)}{\pi}D_{gq}(z)\right\} \qquad \left[z = \frac{\tau_\mu}{\tau}\right]$$

$$D_{qq}(z) = -P_{qq}(z)\log\frac{\mu_F^2 z}{M^2_{\mu\mu}} + C_F\left\{2\left[\frac{\pi^2}{6}-2\right]\delta(1-z) + 2(1+z^2)\left(\frac{\log(1-z)}{1-z}\right)_+\right\} - f_{qq}(z)$$

$$D_{gq}(z) = -\frac{1}{2}P_{qg}(z)\log\frac{\mu_F^2 z}{M^2_{\mu\mu}(1-z)^2} + \frac{T_R}{4}(1+6z-7z^2) - f_{qg}(z)$$

$$\frac{d\mathcal{L}^{gq}}{d\tau} = \int_\tau^1 \frac{dx}{x}\left[q(x,\mu_F^2)g\left(\frac{\tau}{x},\mu_F^2\right) + g(x,\mu_F^2)q\left(\frac{\tau}{x},\mu_F^2\right)\right]$$

In compl. analogy the foll. processes can be treated due to the fact. theorem:

$p_1p_2 \to W^\pm, Z + X \qquad p_1p_2 \to \tilde\ell\bar{\tilde\ell} + X \qquad p_1p_2 \to nj + X$

§9. $e^+e^- \to$ hadrons: total cxn

parton picture:

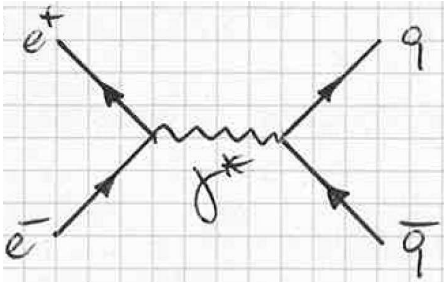

$$\sigma_0 = \frac{4\pi\alpha^2}{3s}\; N_c e_q^2$$

QCD: virt. corr.

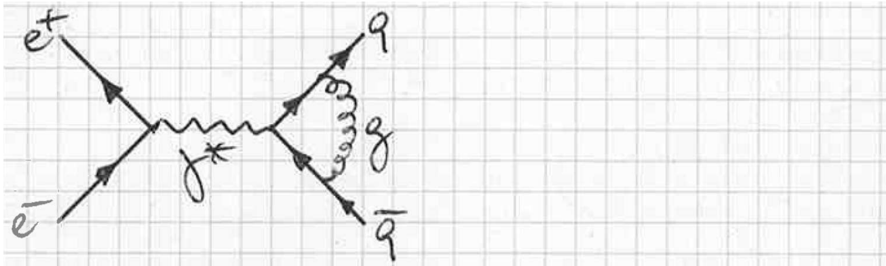

real corr.

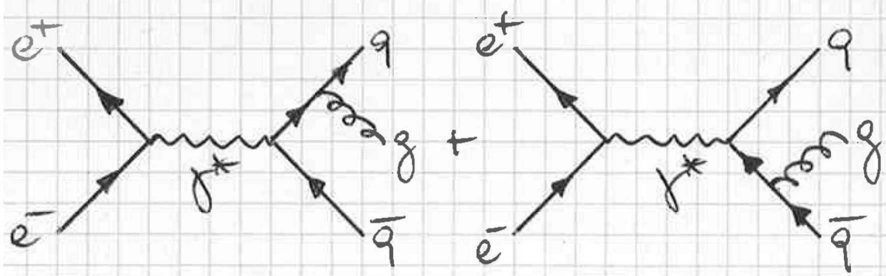

$$\begin{aligned}
\sigma &= (1 + \delta_V + \delta_R)\; \sigma_0 \\
\delta_V &= C_F \frac{\alpha_s}{\pi} \Gamma(1+\epsilon) \left(\frac{4\pi\mu^2}{s}\right)^{\epsilon} \left\{ -\frac{1}{\epsilon^2} - \frac{3}{2\epsilon} - 4 + \frac{2}{3}\pi^2 + \mathcal{O}(\epsilon) \right\} \\
\delta_R &= C_F \frac{\alpha_s}{\pi} \Gamma(1+\epsilon) \left(\frac{4\pi\mu^2}{s}\right)^{\epsilon} \left\{ \frac{1}{\epsilon^2} + \frac{3}{2\epsilon} + \frac{19}{4} - \frac{2}{3}\pi^2 + \mathcal{O}(\epsilon) \right\}
\end{aligned}$$

total cxn: $\sigma = \left(1 + \frac{3}{4} C_F \frac{\alpha_s}{\pi}\right) \sigma_0 = \left(1 + \frac{\alpha_s}{\pi}\right) \sigma_0$

$$R\text{-value} = \frac{\sigma(e^+e^- \to had)}{\sigma(e^+e^- \to \mu^+\mu^-)} : \quad R_B = 3\sum_q e_q^2$$

[known at N^{4}LO]

$$R = R_B \left[1 + \frac{\alpha_s}{\pi} + \sum_{n\geq 2} c_n \left(\frac{\alpha_s}{\pi}\right)^n \right] \quad \text{for } \overline{MS} \text{ @ } \mu^2 = s$$

$$c_2 = \frac{365}{24} - 11\zeta(3) - \left(\frac{11}{12} - \frac{2}{3}\zeta(3)\right) N_F \approx 1.986 - 0.115 N_F$$

$$\begin{aligned} c_3 = {} & \frac{87029}{288} - \frac{1103}{4}\zeta(3) + \frac{275}{6}\zeta(5) \\ & - \left(\frac{7847}{216} - \frac{262}{9}\zeta(3) + \frac{25}{9}\zeta(5)\right) N_F \\ & + \left(\frac{151}{162} - \frac{19}{27}\zeta(3)\right) N_F^2 \\ & - \frac{1}{72}\zeta(2)(33 - 2N_F)^2 + \eta \left(\frac{55}{72} - \frac{5}{3}\zeta(3)\right) \\ & \approx -6.637 - 1.200 N_F - 0.005 N_F^2 - 1.240\eta \end{aligned}$$

$$\eta = \frac{(\sum e_q)^2}{3\sum e_q^2}$$

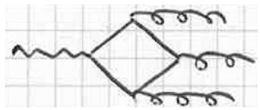

high precision determination of $\alpha_s(M_Z^2)^{\overline{MS}}_{(5)} = 0.122 \pm 0.003$

§10. Jets in QCD

asympt. freedom: In the femto-universe $d \lesssim 10^{-15}$ cm strongly interacting processes proceed as one quantum processes on the level of quarks and gluons. [$\to$ analogous to e and γ in QED]

Jet hypothesis: Parton configurations built up in the femto-universe transform at large distances $d \gtrsim 10^{-13}$ cm into bundles of hadrons with limited transverse momentum $p_\perp \lesssim 500$ MeV $\equiv$ jets

$\Rightarrow$ jet analyses: tests of QCD in femto-universe

jet structure: determined by (non-)perturbative QCD

(a) 0th order QCD: $e^+e^- \to q\bar{q}$

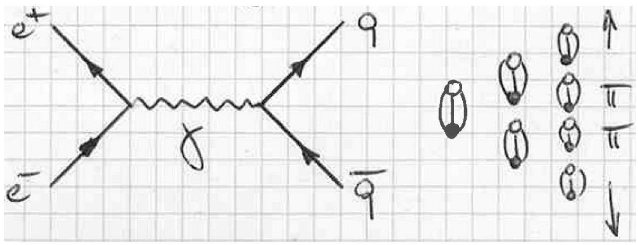

energy flux tube: spont. $q\bar{q}$ production $\Rightarrow$ break up of flux tube with small $p_\perp$

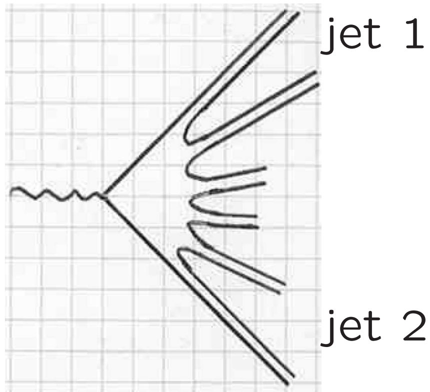

"SPEAR"-Jets

(b) gluon jets in e^+e^- annihilation:

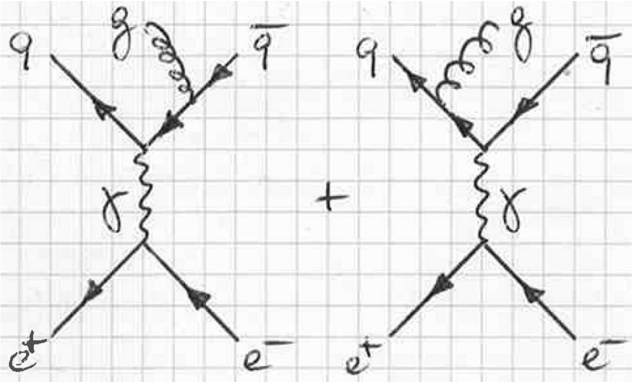

acceleration of color charge $\Rightarrow$ radiation of gluonic gauge quanta [$\sim \gamma$ radiation off accelerated charges]

$q\bar{q}$ kinematics: $x_i = \dfrac{E_i}{\sqrt{s}/2}$

with $x_q + x_{\bar{q}} + x_g = 2$

$0 \leq x_i \leq 1$

$x_q + x_{\bar{q}} = 2 - x_g \geq 1$

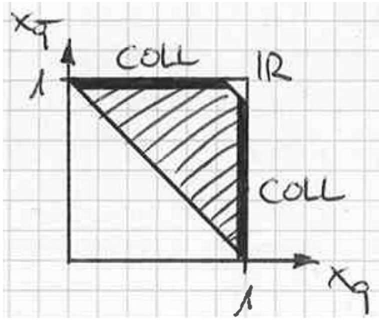

Dalitz plot

pole for $(q+g)^2 = (Q-\bar{q})^2 = Q^2 - 2Q\bar{q} = Q^2(1-x_{\bar{q}})$

$(\bar{q}+g)^2 = Q^2(1-x_q) \qquad [Q = e^+ + e^- = \sqrt{s}(1;\vec{0})]$

$$\boxed{\frac{1}{\sigma_{q\bar{q}}}\frac{d\sigma}{dx_q dx_{\bar{q}}} = \frac{2}{3}\,\frac{\alpha_s}{\pi}\,\frac{x_q^2 + x_{\bar{q}}^2}{(1-x_q)(1-x_{\bar{q}})}}$$

$x_q \to 1 : g \parallel \bar{q}$ coll. conf.
$x_{\bar{q}} \to 1 : g \parallel q$
$x_q, x_{\bar{q}} \to 1 : x_g \to 0$ infrared

Exp. development: Increase of energy $\Rightarrow$
- jets become broader
- clear 3-jet events: PETRA-jets $\leftarrow$ visible QCD gauge quanta

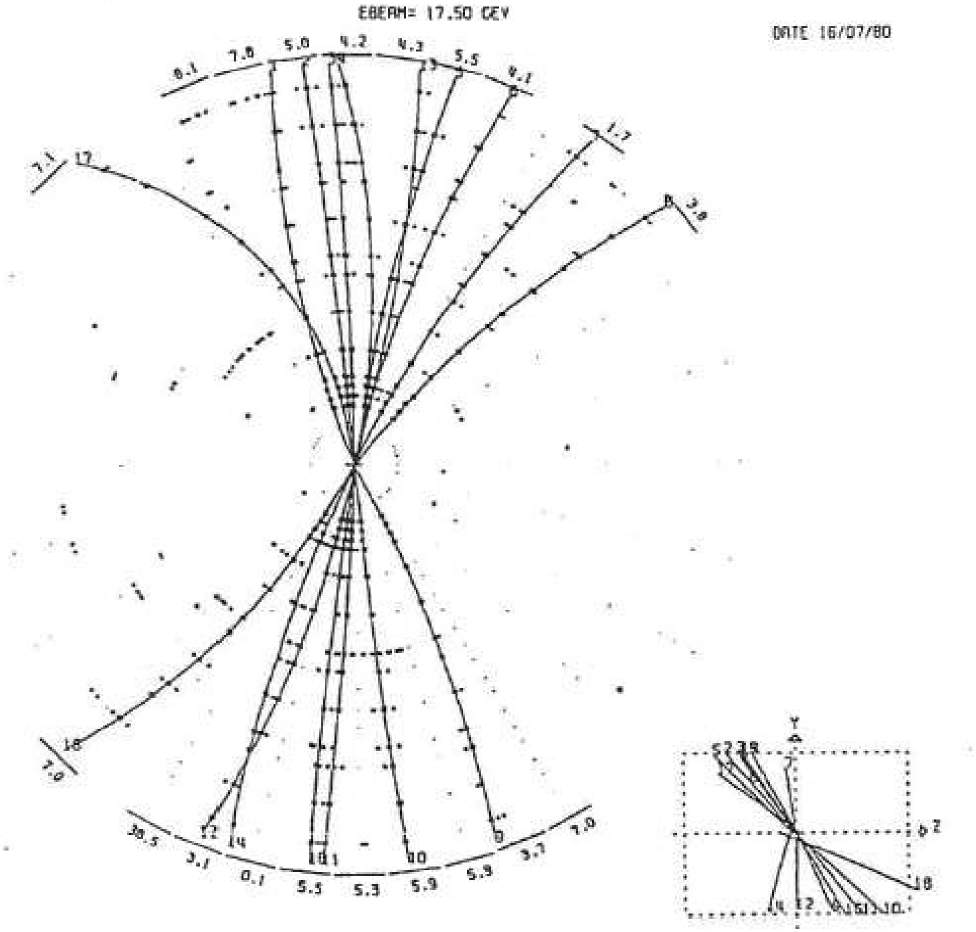

Fig. 29 A two-jet events as observed at W = 35 GeV in the TASSO detector.

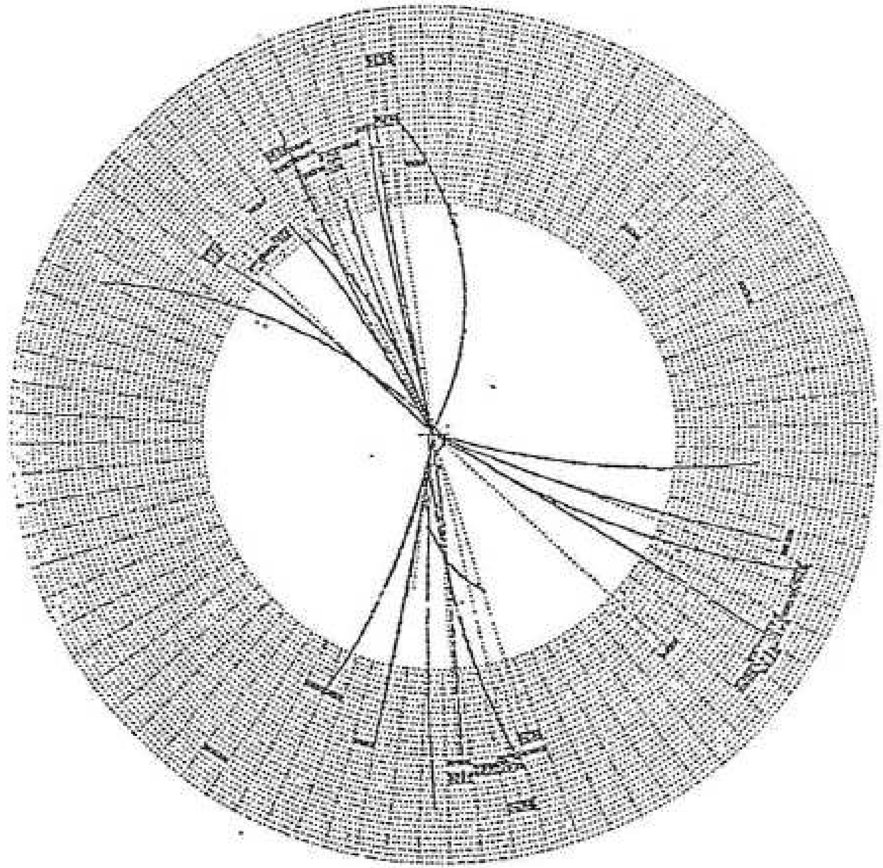

Fig. 11.12 A three-jet event observed by the JADE detector at PETRA.

- measurement of gluon spin:

$$s_g = 1 \Rightarrow \rho_1 \sim \frac{1}{(1-x_q)(1-x_{\bar{q}})} \qquad \text{div. for } x_g \to 0; x_q, x_{\bar{q}} \to 1$$

$$s_g = 0 \Rightarrow \rho_0 \sim \frac{x_g^2}{(1-x_q)(1-x_{\bar{q}})} \qquad \text{finite for } x_g \to 0$$

- measurement of gluon color: 4-jet events:

$$\chi = \angle(E_{12}, E_{34}) :$$

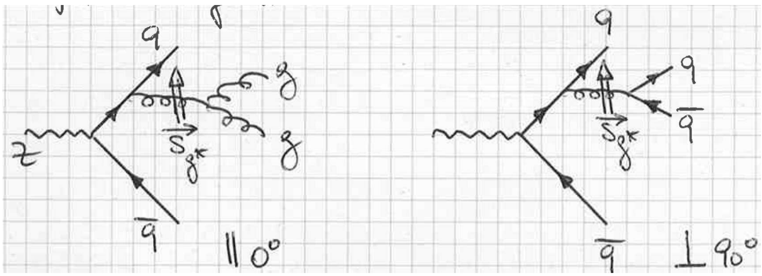

$$gg = \frac{(1-z+z^2)^2}{z(1-z)} + z(1-z)\cos 2\chi$$

$$q'\bar{q}' = \frac{1}{2}[z^2 + (1-z)^2] - z(1-z)\cos 2\chi$$

$$SU_3 : 0° \text{ vs. } U_1 : 90°$$

- jet multiplicity: $f_n(y) =$ fraction of events with n jets in final state:

$$\sum f_n(y) = 1 \qquad y = \text{max. jet mass: } M_{jet}^2 \leq ys$$

$$f_{n+2}(y) = \left(\frac{\alpha_s}{2\pi}\right)^n \sum_{j=0}^{\infty} C_{nj}(y) \left(\frac{\alpha_s}{2\pi}\right)^j \quad \Rightarrow \text{measurement of } \alpha_s$$

Ex.: 2- and 3-jet distributions:

$$f_3 = \int_{(p_i+p_j)^2 \geq ys} dx_1 dx_2 \, \frac{2}{3} \, \frac{\alpha_s}{\pi} \, \frac{x_1^2 + x_2^2}{(1-x_1)(1-x_2)}$$

$$= \frac{2}{3} \, \frac{\alpha_s}{\pi} \left[(3-6y)\log\frac{y}{1-2y} + 2\log^2\frac{y}{1-y} + \frac{5}{2} - 6y - \frac{9}{2}y^2 + 4Li_2\left(\frac{y}{1-y}\right) - \frac{\pi^2}{3} \right]$$

$$f_2 = 1 - f_3 \qquad Li_2(x) = -\int_0^x \frac{dy}{y}\log(1-y) = \sum \frac{x^n}{n^2} \text{ for } |x| \leq 1$$

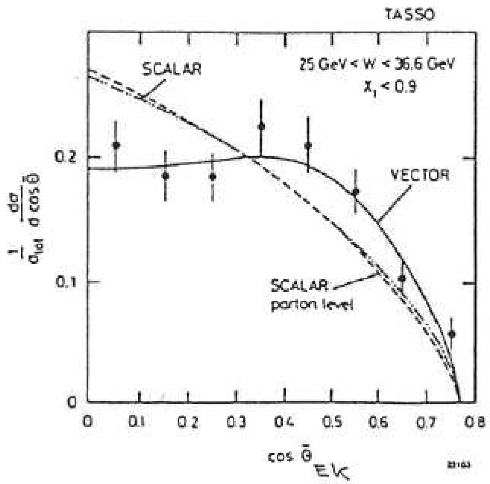

Fig. 7.25
The cosθ distribution of events with $x_1 < 0.9$. The solid line and the dashed-dotted line show the distribution predicted for vector gluons and scalar gluons respectively. The predictions include hadronization. For comparison the prediction for a scalar gluon on the parton level is shown in Fig. 7.24. The distributions are normalized to the number of observed events. EK = Ellis - Kan Ciner

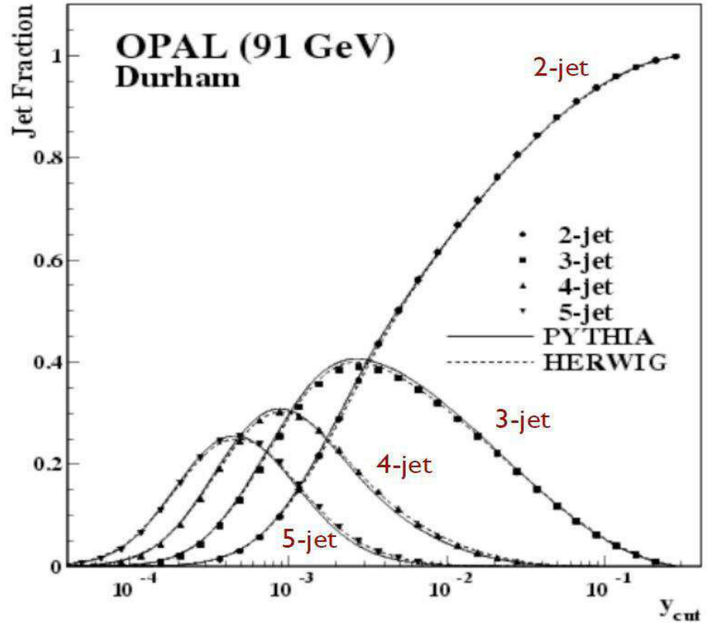

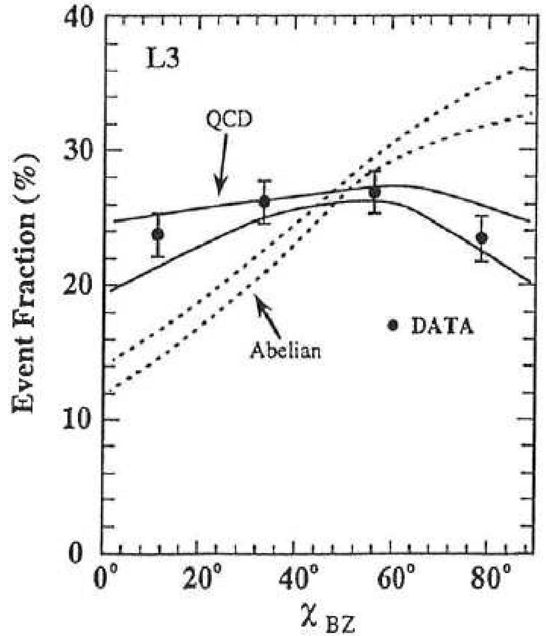

Fig. 3.11. Distribution in the Bengtsson-Zerwas angle at LEP. Figure from ref. [26].

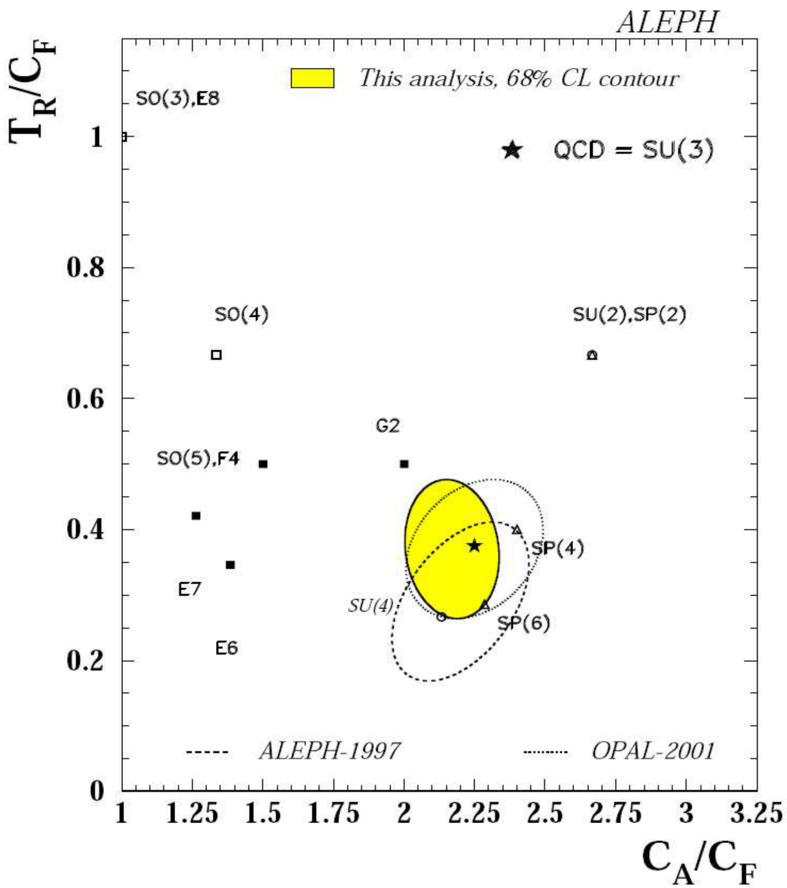

(c) jets in high-energy $p\bar{p}$ scattering at large transv. mom.

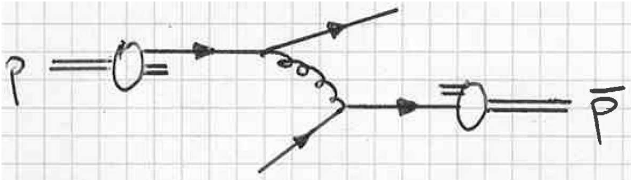

large $p_\perp$ in subsystem $\Rightarrow$ small space-time distance for scattering process

Rutherford process: $q + q \to q + q, q + \bar{q} \to q + \bar{q}$

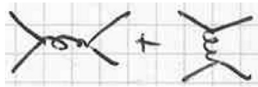

Compton scattering: $g + q \to g + q, g + \bar{q} \to g + \bar{q}$

annihilation: $q + \bar{q} \to g + g$

gluon fusion: $g + g \to q + \bar{q}$

gluon scattering: $g + g \to g + g$

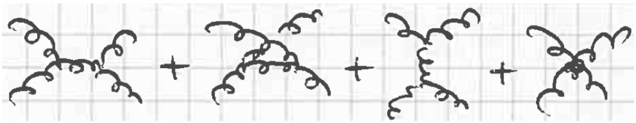

• detection of Rutherford scattering in quark-gluon sector:

$$\frac{d\sigma^R}{d\cos\theta} \sim \frac{1}{\sin^4 \frac{\theta}{2}} \sim \frac{1}{(1-\cos\theta)^2} \text{ strongly increasing for } \theta \to 0$$

$$\chi = \frac{1+\cos\theta}{1-\cos\theta} \quad d\chi \sim \frac{d\cos\theta}{(1-\cos\theta)^2} \Rightarrow \underline{\underline{\frac{d\sigma^R}{d\chi} = \text{flat}}}$$

modulo: χ-dependence in $d\sigma^R$

Q^2-dependence in $\alpha_s(Q^2)$, quark densities

Tabelle 20-1 Die Querschnitte für die möglichen Parton-Parton-2-Teilchen-Reaktionen in führender Ordnung in α_s. Dabei numerieren wir mit i, j $(1 \leq i,\ j \leq f)$ die verschiedenen Quark-Flavors durch (s. Gl. (19-2)).

Reaktion	Streuquerschnitt $\frac{\hat{s}^2}{\pi \alpha_s^2} \frac{d\sigma}{d\hat{t}}$
$q^i + q^j \to q^i + q^j \quad (i \neq j)$ $q^i + \bar{q}^j \to q^i + \bar{q}^j \quad (i \neq j)$	$\frac{4}{9} \frac{\hat{s}^2 + \hat{u}^2}{\hat{t}^2}$
$q^i + q^i \to q^i + q^i$	$\frac{4}{9} \left(\frac{\hat{s}^2 + \hat{u}^2}{\hat{t}^2} + \frac{\hat{s}^2 + \hat{t}^2}{\hat{u}^2} \right) - \frac{8}{27} \frac{\hat{s}^2}{\hat{u}\hat{t}}$
$q^i + \bar{q}^i \to q^j + \bar{q}^j \quad (i \neq j)$	$\frac{4}{9} \frac{\hat{t}^2 + \hat{u}^2}{\hat{s}^2}$
$q^i + \bar{q}^i \to q^i + \bar{q}^i$	$\frac{4}{9} \left(\frac{\hat{s}^2 + \hat{u}^2}{\hat{t}^2} + \frac{\hat{t}^2 + \hat{u}^2}{\hat{s}^2} \right) - \frac{8}{27} \frac{\hat{u}^2}{\hat{s}\hat{t}}$
$q^i + \bar{q}^i \to G + G$	$\frac{32}{27} \frac{\hat{u}^2 + \hat{t}^2}{\hat{u}\hat{t}} - \frac{8}{3} \frac{\hat{u}^2 + \hat{t}^2}{\hat{s}^2}$
$G + G \to q^i + \bar{q}^i$	$\frac{1}{6} \frac{\hat{u}^2 + \hat{t}^2}{\hat{u}\hat{t}} - \frac{3}{8} \frac{\hat{u}^2 + \hat{t}^2}{\hat{s}^2}$
$q^i + G \to q^i + G$ $\bar{q}^i + G \to \bar{q}^i + G$	$-\frac{4}{9} \frac{\hat{u}^2 + \hat{s}^2}{\hat{u}\hat{s}} + \frac{\hat{u}^2 + \hat{s}^2}{\hat{t}^2}$
$G + G \to G + G$	$\frac{9}{2} \left(3 - \frac{\hat{u}\hat{t}}{\hat{s}^2} - \frac{\hat{u}\hat{s}}{\hat{t}^2} - \frac{\hat{s}\hat{t}}{\hat{u}^2} \right)$

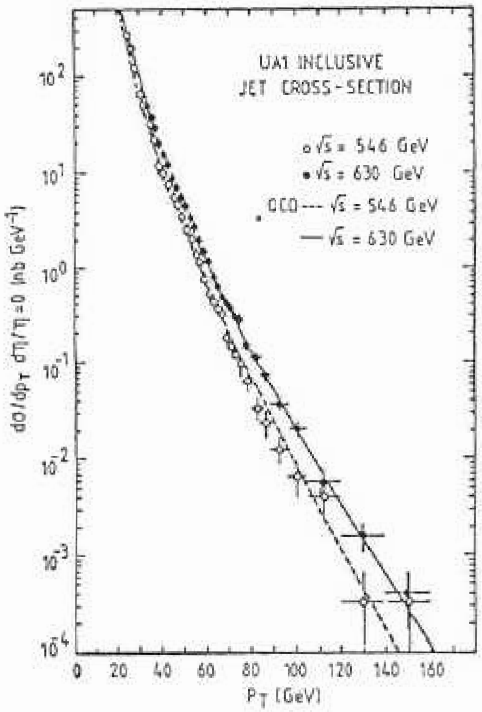

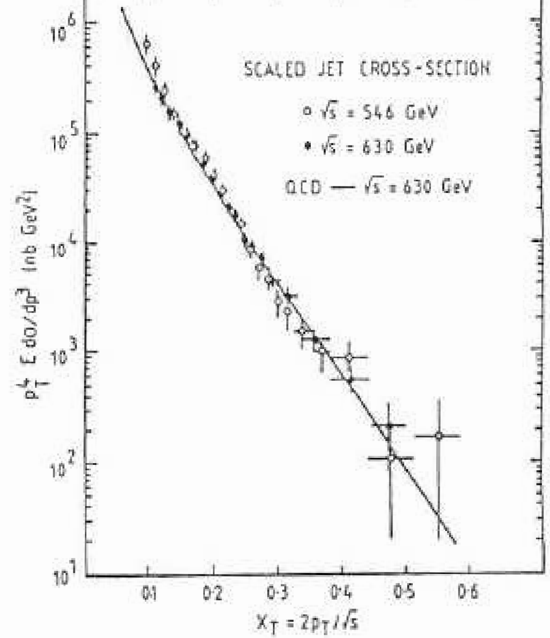

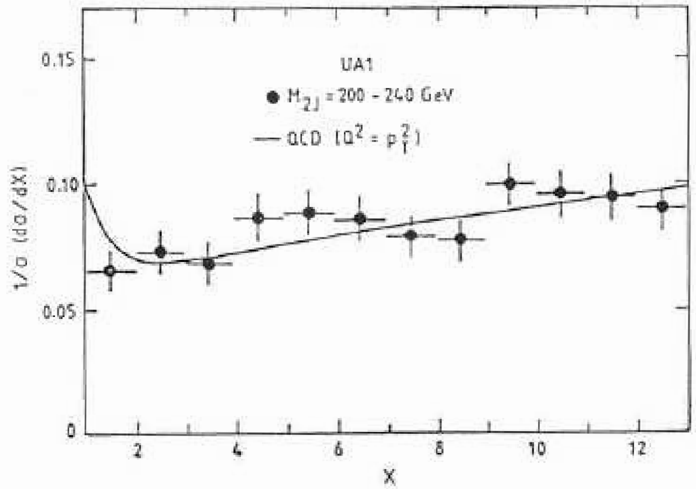

(d) quarkonium decays

$\rho^0 = \frac{1}{\sqrt{2}}(u\bar{u} - d\bar{d})$

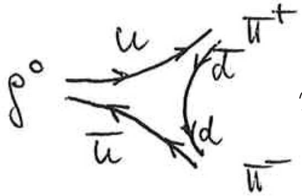

$m_\rho > 2m_\pi$ Zweig-allowed decay ⇒ large width

$\Psi = c\bar{c}$ (3097)

$\Upsilon = b\bar{b}$ (9460)

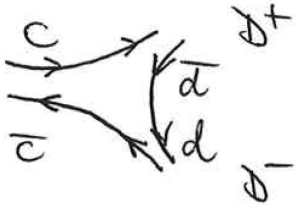

$m_\Psi < 2m_D$ Zweig-allowed decay not possible

• leptonic decays: $\Psi \to e^+e^-, \mu^+\mu^-$ $[q\bar{q}]$

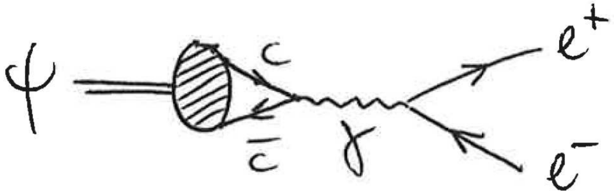

$$\Gamma(\Psi \to \ell^+\ell^-) = \frac{16\pi\alpha^2}{m_\Psi^2} Q_c^2 |\phi(0)|^2 \quad [\leftarrow \text{positronium}]$$

+2/3 ↑ ↑ wave func. @ origin [NR]

• hadronic decays: quarkonia for which Zweig-allowed decays are impossible decay into gluons → jets at high energies [$\Upsilon, \ldots$]

$1^{--} \not\to gg$: lowest ortho-channel

[Yang]

$$\Psi = c\bar{c} \to 3g$$
$$\Upsilon = b\bar{b} \to 3g$$

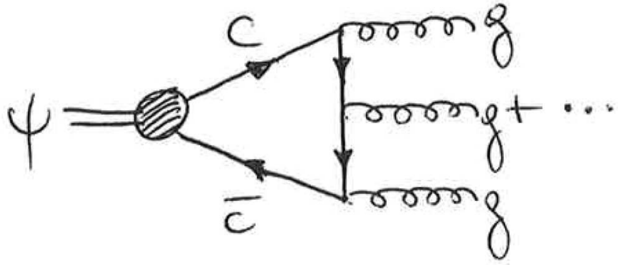

annihilation distance: $d \sim m_Q^{-1} \ll 1$ fm $\Rightarrow$ asympt. freedom

<u>width:</u> $\Gamma(Q\bar{Q} \to ggg) = \dfrac{160}{81}(\pi^2 - 9)\dfrac{\alpha_s^3(M^2)}{M^2}|\phi_s(0)|^2$

$\Psi = (0.05 \pm 0.01)$ MeV

$\Upsilon = 0.04$ MeV

quarkonia are very narrow resonances [$\leftarrow$ asympt. freedom]

<u>Dalitz:</u> $\dfrac{1}{\Gamma}\dfrac{d\Gamma}{dx_1 dx_2} = \dfrac{6}{\pi^2 - 9}\;\dfrac{x_1^2(1-x_1)^2 + x_2^2(1-x_2)^2 + x_3^2(1-x_3)^2}{x_1^2 x_2^2 x_3^2}$

<u>color charge of gluons:</u>

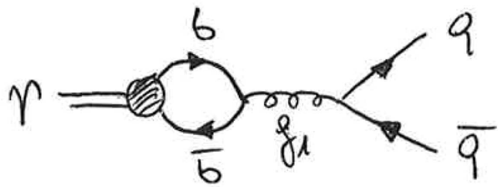

if g were a $U(1)$ gauge field the dominant decay mode would be $\Upsilon \to g_{virt} \to q\bar{q}$

$\Rightarrow$ 2 jet final states = off

not observed $\Rightarrow$ $\boxed{\mathcal{C}[g] \neq 0}$

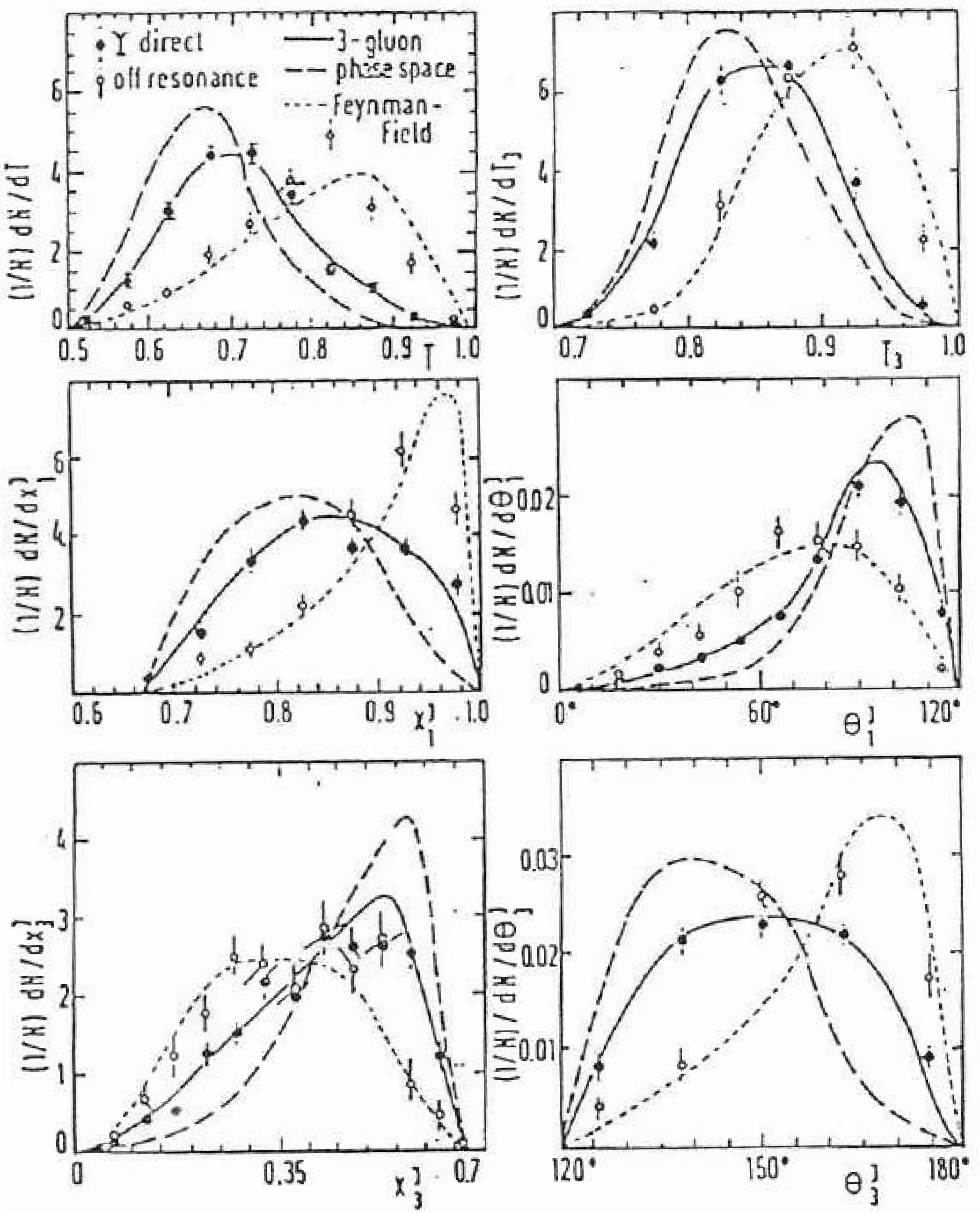

Fig. 2 Experimental distributions of thrust T, triplicity T_3 reconstructed gluon energies x_1^J, x_3^J and reconstructed angles θ_1^J, θ_3^J between gluons compared to Monte-Carlo calculations based on various models.